Surface Structures and Segregation of Polystyrene/Poly(methyl methacrylate) Blends Studied by Sum-Frequency (SF) Spectroscopy

Yi Liu[†] **and Marie C. Messmer***

Department of Chemistry, Lehigh University, 7 Asa Drive, Bethlehem, Pennsylvania 18015

Received: December 17, 2002; In Final Form: April 9, 2003

Molecular structures at the surface and interface of polystyrene (PS)/poly(methyl methacrylate) (PMMA) blend films were obtained by sum-frequency (SF) spectroscopy. Using this technique, both the surface of the blend and the internal interface between the two blend polymers are simultaneously probed. Two types of blend film structures were obtained depending on sample treatment. The as-cast film (dried under vacuum at room temperature) gave a PMMA-on-PS bilayer structure whose SF spectrum was dominated by the C−H symmetric stretch of the PMMA ester methyl groups. When the bulk PMMA concentration was higher than 13% w/w, the SF features were identical to that of the pure PMMA films. The lack of PS SF features in this blend film suggests that the PS phenyl rings may be randomly oriented at the PS−PMMA interface. Upon annealing at 150 °C for 20 h, the PS segregated to the film surface as a result of its lower surface free energy, and a PS-rich phase was formed near the polymer−air interface, as evidenced by the SF spectroscopy, contact angles, and XPS measurements. However, the SF peak of the ester methyl group was still observed, indicating that the PMMA was still oriented at the PMMA−PS interface.

Introduction

Surface properties of polymer blends have been of great interest in the past decade because they are often very different from that of the bulk material.[1−3] Surface composition of a polymer and/or copolymer blend is primarily controlled by the difference in surface free energy (γ) of each component, molecular weight, end groups, architecture, and tacticity. The component with a lower γ often segregates to the free (air or vacuum) polymer surface to minimize the interfacial free energy.[3] A comprehensive understanding about the surface and interface of polymer blends is critical in controlling many important surface properties such as wettability, adhesion, friction, and biocompatibility. As a model for the investigation of immiscible polymer blends, the polystyrene (PS)/poly(methyl methacrylate) (PMMA) pair has been the focus of many studies. The chemical structures of PS and PMMA are shown in Figure 1. The surface properties of PS/PMMA blends have been extensively characterized using XPS, AFM/LFM, and neutron reflectivity. It is known that PS molecules preferentially segregate at the free surface under equilibrium conditions because PS has a lower surface free energy than PMMA.[4−6] However, the surface component and morphology vary depending on other factors. For example, in a blend film of high-molecular-weight PS and low-molecular-weight PMMA, the latter can be stable at the blend surface as result of reduced conformational entropic penalty.[7] The end groups and film thickness also affect surface segregation and morphology.[4,6,8,9] The surface structure of a PS/PMMA blend film is also influenced by solvents[10] and annealing.[5,8,10,11] By choosing a proper solvent and/or annealing at a temperature higher than the glassy transition temperatures of PS and PMMA, one can manipulate the surface structures of PS/PMMA blend films. Although much progress has been made in acquiring knowledge about the PS/PMMA blend surface and interface through the use of surface-sensitive techniques, many details at the molecular level are not fully elucidated. For example, what orientation does a functional group adopt at the polymer−air, polymer−liquid, and polymer−polymer interface? Because the thickness of the surface and interface that controls the polymer properties is typically in the nanometer range, the analytical method must have high interfacial selectivity to gain in-depth information about the blend film surface. Ideally, the method should also be in situ capable because the polymer surface often reconstructs upon changes in its environmental conditions.[12]

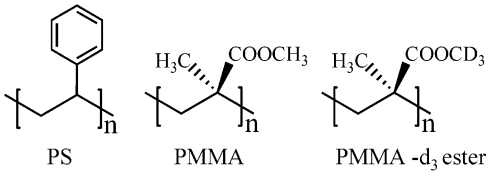

Figure 1. Chemical structures of the polymers used in this study.

In recent years, sum-frequency (SF) spectroscopy has been applied for the investigation of polymer surface and interface.[13] It has been demonstrated that the reflected SF signals are most likely from the polymer surfaces rather than from the bulk[14,15] or substrate−polymer interface.[16,17] A variety of polymers,[14,16,18−24] copolymers,[25−27] and polymer blends[17,28] have been examined by SF spectroscopy. The SF studies of polymer−polymer interface have only recently been reported.[29−31] The theory of sum-frequency generation (SFG) has been described in detail in a number of reviews.[32−35] As a result of its second-order dependence on the input field, SFG is forbidden in media possessing inversion symmetry within the electric-dipole approximation but allowed at an interface where the inversion symmetry is broken. Therefore, SF spectroscopy is highly interface-sensitive and in situ capable. Another key advantage

* Corresponding author. Tel: 610-758-3674. Fax: 610-758-6555. E-mail: mcm6@lehigh.edu.

[†] Current address: Department of Chemistry & Biochemistry, University of Delaware, 173 Brown Lab, Newark, DE 19716.

10.1021/jp0277513 CCC: $25.00
Published on Web 08/13/2003

of SF spectroscopy is that it provides information about the orientation of molecules by choosing proper polarization combinations of the incoming IR and visible beams and the output SF beams.[36−38] The ssp polarization combination, with the polarization listed in the order of sum-frequency, visible, and IR, provides information about the transition dipole moment perpendicular to the surface. The sps polarization combination probes modes that have IR transition moments in the plane of interface. The ppp polarization probes all the components of the allowed vibrations. The surface sensitivity of SF spectroscopy has also been demonstrated to be in the submonolayer range.[15,39]

In this work, we extend SF spectroscopy to the study of surface structures and segregation of ultrathin PS/PMMA blend films (thickness < 80 nm). The segregation process of PS/PMMA before and after annealing was also monitored by XPS and contact-angle measurements, and comparison of these with the SF results is discussed.

Experimental Section

Materials. Poly(methyl methacrylate) (M_w ca. 120 000, T_g = 114 °C), polystyrene (M_w ca. 212 400, T_g = 100 °C), and chloroform (99.9%) were purchased from Aldrich and were used without further purification. Deuterated PMMA-d_3 ester ($[-CH_2C(CH_3)(CO_2CD_3)-]_n$, M_n ca. 28 700) was purchased from Polymer Source. Sulfuric acid and hydrogen peroxide were analytical grade and obtained from EM Science. Deionized (DI) water was obtained with Barnstead NANOpure system until final resistivity >16.0 mΩ/cm was reached. Glass plates, HPLC grade acetone (99.6%), and methanol (99.9%) were purchased from Fisher Scientific.

Sample Preparation. Glass plates were cut into 25 × 25 mm slides, were soaked in methanol for 30 min, and rinsed with copious amount of DI water. The slides were then immersed in piranha solution (7:3 concentrated H_2SO_4/30% H_2O_2) for 1.5 h at ~110 °C. ***Caution****: Piranha solution is a highly reactive mixture and severely exothermic during reaction. It should be kept out of contact with oxidizable organic material.* After rinsing with copious amount of water, the slides were dried with nitrogen and heated at 75 °C for 1−3 h. The cleaned glass slides were wetted by water and were featureless in the region from 2800 to 3100 cm^{-1} when examined by SF spectroscopy.

Polymer thin films were typically prepared by spin-coating from a 1.0% solution in $CHCl_3$ at a rate of 3000 rpm for 60 s. A series of PS/PMMA blend films with various bulk concentrations of PMMA were prepared by spin-coating a 1.0% polymer solution in $CHCl_3$ on the substrates and drying under vacuum at room temperature for 12 h. The blend films thus prepared are referred to as "RT-dried" samples. The annealing of samples was carried out in a vacuum at 150 °C for 20 h.

Sum-Frequency Generation. The experimental setup for SFG has been described previously.[40] Briefly, a lithium niobate ($LiNbO_3$) optical parametric oscillator (OPO) was pumped with a Surelite I (Continuum) Nd^{3+}:YAG laser using relay imaging. Tunable IR light was generated between 2600 and 3200 cm^{-1} (3.1−3.8 μm) with a pulse width of 7 ns. The wavelength was calibrated with a polystyrene reference standard. The visible beam at 532 nm used in the sum-frequency experiment was generated with a potassium dihydrogen phosphate (KDP) crystal. The polarization of the IR beam was controlled with a Soleil-Babinet compensator. SF spectra were obtained by using a total internal reflection (TIR) geometry[41,42] in which both the IR and the visible light overlapped at the surface through the glass substrate. A schematic representation of the TIR SFG setup is shown in Figure 2. Although SF signal enhancement has been observed for TIR geometry,[43] it should be noted that the intensity is very sensitive to the incident angles of the laser beams. The IR and visible beams were combined through a coupling prism to the glass substrate with an index-matching liquid. The generated SF light was collected and passed through several collimating optics, absorptive, interference and holographic filters, and a Glan-Taylor polarizer. The signal was detected with a photomultiplier tube and then passed to a preamplifier and gated electronics. Data were collected at 2 or 4 cm^{-1} increments in the region from 2800 to 3100 cm^{-1} using a custom written LabVIEW program, and each point was the average of at least 200 laser shots. Spectra were corrected for the wavelength dependence of the Fresnel factors of the input infrared beam for the small refractive index change in the substrate. Each spectrum is representative of spectra taken from several places on the sample surface.

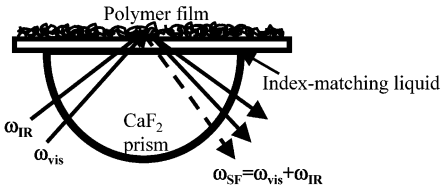

Figure 2. Schematic diagram of the experimental setup for total internal reflection (TIR) SFG.

TABLE 1: C 1s Binding Energy on Pure PMMA and PS Films[44]

		binding energy (eV)			
name	molecular structure	a	b	c	d
PMMA	$-{}^aCH_2{}^bC({}^aCH_3)({}^dCO_2{}^cCH_3)-$	285.00	285.72	286.79	289.03
PS	$-{}^bCH_2{}^bCH({}^aC_6H_5)-$	284.76	285.00		

Contact-Angle Measurements. Advancing contact angles (θ_a) of water (pH 7) were measured at room temperature and ambient humidity with a home-built contact angle goniometer. A Gilmont syringe with a blunt-tip needle was used to deliver water. At least three different areas on the polymer film were measured. Each of the reported θ_a values is an average of at least 10 measurements taken within 20 s of applying each drop of water, and the errors indicate the 95% confidence level.

X-ray Photoelectron Spectroscopy (XPS). Angle dependent XPS experiments were performed on the same series of PS/PMMA blends after SF measurements. XPS data were acquired with a Scienta ESCA 300 using monochromatic Al Kα X-rays. The analysis area of each sample was approximately 0.8 mm^2, and the pass energy of the detector was 150 eV. The pressure of the chamber was approximately 5 × 10^{-9} Torr. The samples were analyzed at electron takeoff angles of 90° and 10° with respect to the surface plane. For high-resolution spectra, six scans of the data were taken for C 1s in the binding energy region from 280 to 300 eV. The binding energies of various carbon atoms of pure PS and PMMA are listed in Table 1.[44] The spectra were charge referenced to the $-C_6H_5$ peak at 285.0 eV and were fitted using a Voigt function with a linear background in the 288.0−297.0 eV and Shirley background in the 282.0−288.0 eV region using the Scienta software. The integrated peak area was divided by atomic sensitivity factors provided in the Scienta software. The carbonyl carbon in ester group at 289.0 eV was chosen as an indicator of PMMA molecules because it is solely contributed from PMMA and does not significantly overlap with other peaks. The near surface mole

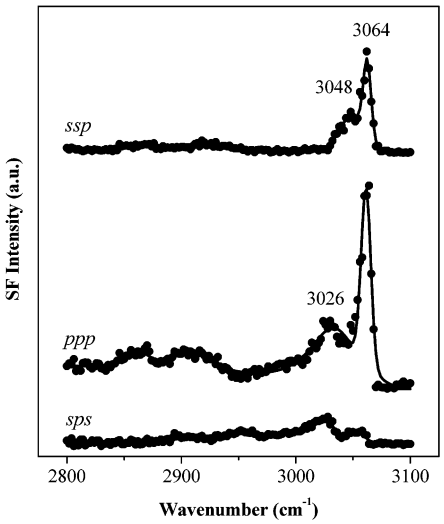

Figure 3. Sum-frequency spectra of polystyrene. The spectra are offset for clarity. The solid lines are fits to the data using Voigt line shapes.

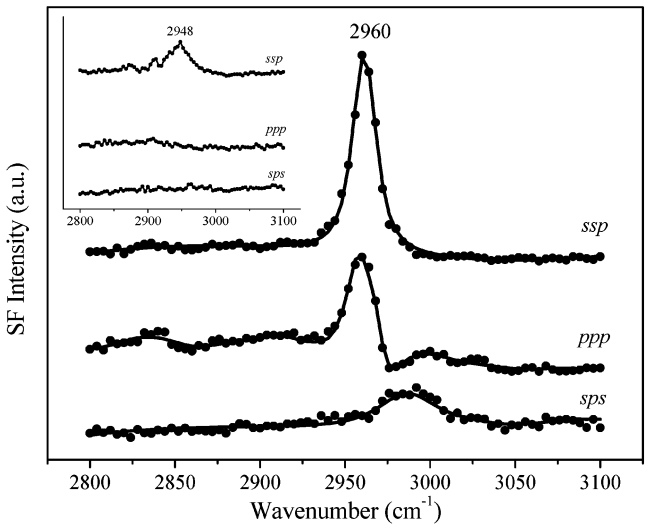

Figure 4. Sum-frequency spectra of PMMA. The spectra are offset for clarity. The solid lines are fits to the data using Voigt line shapes. The inset is the same spectra of the PMMA-d_3 ester.

fraction of PMMA, q, can then be calculated from[5]

$$q = \frac{8R}{1 + 3R} \tag{1}$$

where R is the atom ratio of the ester carbonyl carbon to the total carbon. Some of our polymer blends were thin enough to expose the substrate Si 2p signals, and their film thickness can be estimated as follows. Assuming a thin homogeneous film on a smooth substrate, the XPS intensity from the substrate is given by[45]

$$\ln[I(\beta)] - \ln[I_c(\beta)] = \frac{-d}{\lambda \cos \beta} \tag{2}$$

where β is the angle of the detector with respect to the surface normal, $I(\beta)$ is the photoelectron intensity from the substrate covered by the film, $I_c(\beta)$ is the photoelectron intensity from the bare substrate, d is the thickness of the film, and λ is the escape depth of photoelectrons from the substrate. The intensities of Si 2p from a series of PS films with known thickness on Si wafer were collected at a 90° takeoff angle ($\beta = 0°$), and a calibration curve was plotted using eq 2, from which the film thickness of PS/PMMA blends can be obtained. The average film thickness of the PS/PMMA blends was determined to be ~20 nm. Under these experimental conditions, the analytical depth that can be probed by 90° and 10° takeoff angles were 23 and 4 nm, respectively.

Results and Discussion

PS−Air and PMMA−Air Interface. Before multicomponent polymer systems such as polymer blends are probed by SF spectroscopy, it is important to clarify the characteristic SF features at the homopolymer−air interfaces. The SF spectra of PS in the C−H stretching region are shown in Figure 3. These spectra are qualitatively comparable to those reported in the literature.[19] In both ssp and ppp polarization spectra, the strongest peak occurs at ~3064 cm^{-1} and is assigned to the ν_2 vibrational mode of the phenyl ring. Under a total internal reflection geometry where the 532 nm visible beam was set close to the critical angle of the polymer−air interface, it is believed that the SF signals are mainly from the PS−air interface rather than the PS−substrate interface, and the phenyl groups tend to oriented toward the surface normal.[16−18,46]

Sum-frequency spectra of PMMA in the C−H stretching region are shown in Figure 4. Under the ssp polarization combination, a strong peak at ~2960 cm^{-1} appears. Under ppp polarization, a dip after 2960 peak was observed, probably as a result of the interferences among the various nonzero nonlinear susceptibility components. In the sps spectrum, a relatively weak and broad band around 2986 cm^{-1} was observed. From the literature values of the characteristic IR absorption frequencies of PMMA,[47] the region around 2960 cm^{-1} could be assigned to one or more of these vibrational modes: $-OCH_3$ symmetric,[48,49] $\alpha-CH_3$ asymmetric,[47,48,50] or CH_2 asymmetric stretching.[47,49] To identify the source of the 2960 cm^{-1} peak, we used the PMMA-d_3 ester (structure shown in Figure 1), which has the same backbone structure of PMMA but a deuterated ester methyl ($-OCD_3$) pendent group. A relatively small peak at ~2948 cm^{-1} was observed under ssp polarization (inset in Figure 4). This peak was assigned to the C−H symmetric and asymmetric stretch of either the α-CH_3 or the CH_2 units or both.[51,52] However, these assignments were considered unreliable by Lipschitz.[47] Nonetheless, no observable SF peak appears at 2960 cm^{-1} under ssp polarization, and the spectra are nearly featureless in the region 2800−3100 cm^{-1} under either ppp or sps polarization. The lack of a peak at 2960 cm^{-1} in the SF spectra of PMMA-d_3 ester confirms the assignment of the 2960 cm^{-1} peak as the C−H symmetric stretching of the ester methyl groups. The assignment of the ester methyl groups has also been performed by Chen and co-workers.[14] They excluded the contributions of the α-CH_3 and methylene asymmetric stretches to the ssp spectrum by comparing theoretical calculated results of asymmetric stretches of methyl and methylene groups with their experimental data. Our results support their earlier assignments. From Figure 4, one can deduce that the $-OCH_3$ groups tend to tilt toward the surface normal, and the α-CH_3 and methylene units are randomly distributed on the PMMA surface.[14] To confirm that the SF signal is from the PMMA−air rather than the PMMA−substrate interface, we collected the SF signal at the same critical angle with a drop of D_2O on top of the PMMA film and no signal was observed, indicating that the SF signal is almost exclusively from the polymer−air interface. This result is consistent with that observed by Chen and co-workers.[14,20]

Sum-frequency spectra of the PS and PMMA films revealed that SF peaks characteristic of these two polymer surfaces are

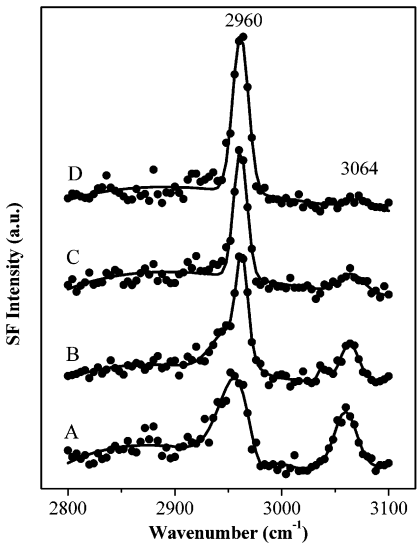

Figure 5. Sum-frequency spectra of RT-dried PS/PMMA blends with various bulk mole fraction of MMA units (f_{MMA}): (A) $f_{MMA} = 0.03$; (B) $f_{MMA} = 0.06$; (C) $f_{MMA} = 0.09$; (D) $f_{MMA} = 0.11$. Spectra were taken with ssp polarization and are offset for clarity. The solid lines are fits to the data using Voigt line shapes.

spectroscopically well-separated. The SF peaks from the PS surface originate from the vibrational modes of the phenyl rings whose C−H stretching frequencies are in the region 3000−3100 cm^{-1}, whereas the peak of PMMA is almost exclusively the C−H symmetric stretching of the ester methyl group centered at 2960 cm^{-1}. Therefore, the interference of these two polymer SF peaks is minimal, which makes it possible to extract more quantitative information from the SF spectra of the PS/PMMA blends.

PS/PMMA Blends. Sum-frequency spectra of a series of RT-dried PS/PMMA blends under ssp polarization are shown in Figure 5. The bulk PMMA concentrations are expressed in terms of mole fraction of PMMA monomer units, f_{MMA}. It can be seen that peaks characteristic of both PS and PMMA appear, and their relative intensities change as f_{MMA} increases. The 2960 cm^{-1} peak originates from the ester methyl group of PMMA, and the 3064 cm^{-1} peak from the symmetric stretch of the phenyl rings on PS. The sps and ppp spectra of PS/PMMA blends were also taken (data not shown). No appreciable peaks were observed for the sps spectra partially because of the scattering of the laser beams within the polymer blends. Nonetheless, it also indicates that there are no significant changes of the orientation of the ester methyl group of PMMA. Assuming no change in orientation, the SF intensity ratio of the PMMA and PS characteristic peaks is indicative of the surface density ratio of the PS and PMMA domains. The relative SF intensity of the PMMA peak increases as a function of f_{MMA}, indicating that the PMMA becomes appreciable at the surface of the blends. The spectra of RT-dried samples with $f_{MMA} = 0.03$ and $f_{MMA} = 0.06$ (A and B in Figure 5) are different from that of the pure PMMA. The widths at the half-height of the peaks in spectrum (A) are much broader than that of pure PMMA (31 vs 17 cm^{-1}), and a shoulder at ~2952 cm^{-1} is obvious in spectrum B and indicates that the features probably originate from the PMMA−PS interface (vide infra). For $f_{MMA} = 0.11$ (D in Figure 5), the spectrum is dominated by PMMA, whereas the PS peaks are much smaller. In fact, for blends with higher f_{MMA}, the spectra were almost identical to the pure PMMA, with no observable PS peaks. This observation suggests that a PMMA overlayer forms on PS. Because the film thickness of our samples is below 23 nm, which is only about twice the radius of gyration of PS, it is reasonable to believe that the blend structure is a PMMA on PS bilayer. This is consistent with the AFM and XPS studies of the same blend system (with higher PMMA content) conducted by Ton-That et al.[5] We have noticed that even for f_{MMA} larger than 0.13 the RT-dried films were still transparent, indicating that there were no significant domains segregated within the blends. The disappearance of SF signals due to PS under both ssp and ppp (not shown) polarization suggests that the phenyl ring orientation becomes more random at the blend surface than at the PS−air interface. The SF studies of PS/poly(butyl methacrylate) showed similar behavior of PS on the blend surface;[17] i.e., the phenyl rings tend to lie along the blend surface.

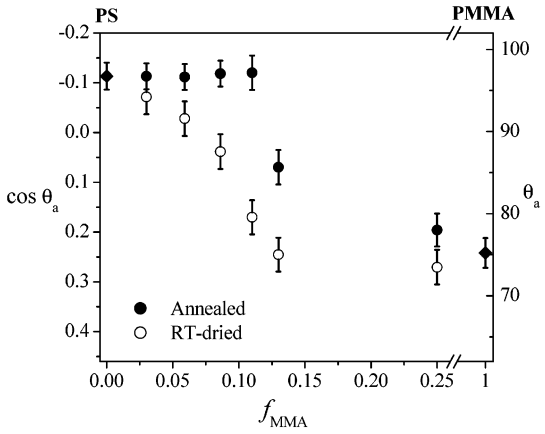

Figure 6. Water contact-angle measurements of PS/PMMA blends with various bulk mole fraction of MMA units (f_{MMA}) before (○) and after (●) annealing. The values of pure PS and PMMA (◆) films are also included for comparison.

To obtain more information about surface properties, the PS/PMMA blends were also examined using water contact-angle measurements, and the results are shown in Figure 6. Water contact angles on thin PS and PMMA films prepared using the same procedure were 97 ± 2° and 76 ± 2°, respectively. The contact angles on the RT-dried PS/PMMA blends decreased as f_{MMA} increased (open circles in Figure 6), consistent with the enrichment of the PMMA molecules at the surface of the PS/PMMA blends, which can be explained in terms of the different solubility of PS and PMMA in $CHCl_3$. Chloroform is a better solvent for PMMA than PS.[5] Therefore, during the spin-coating PS solidifies earlier on the substrate, leaving an enriched PMMA layer on the surface. The contact angle results correlate well with the SF spectra of the RT-dried PS/PMMA blends.

Effect of Annealing. Although the RT-dried PS/PMMA blends were relatively stable under ambient conditions as a result of the low mobility of these two polymers, they are not at their thermodynamic equilibrium state because PS has lower surface free energy than PMMA.[5,6] If the blends were annealed at temperatures higher than the T_g of PS and PMMA, one would expect the PS molecules to populate the polymer−air interface preferentially. Another driving force of the segregation of PS and PMMA in our thin films (~20 nm) might be the stronger affinity of PMMA for the hydrophilic substrate.[53,54] This segregation of PS and PMMA was indeed seen in the SF spectra, contact angles, and XPS measurements of the annealed blend samples. The SF spectra of the annealed PS/PMMA under ssp polarization are shown in Figure 7. The relative intensity of the PS peak with respect to PMMA peak increased dramatically upon annealing, consistent with migration of PS molecules to the blend surface. The SF intensities of the blend with $f_{MMA} = 0.11$ (D in Figure 7) are much smaller than the others. In fact,

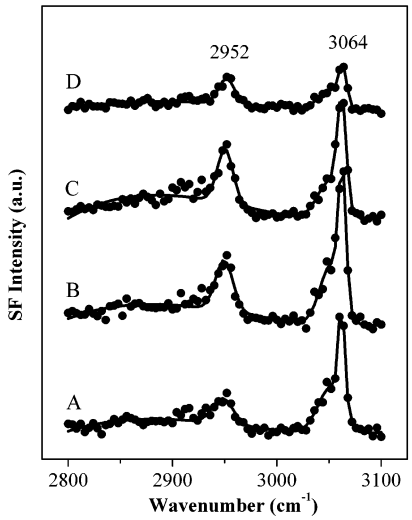

Figure 7. Sum-frequency spectra of annealed PS/PMMA blends with various bulk mole fraction of MMA units (f_{MMA}): (A) $f_{MMA} = 0.03$; (B) $f_{MMA} = 0.06$; (C) $f_{MMA} = 0.09$; (D) $f_{MMA} = 0.11$. Samples were annealed in a vacuum at 150 °C for 20 h. Spectra were taken with ssp polarization and are offset for clarity. The solid lines are fits to the data using Voigt line shapes.

TABLE 2: PMMA Mole Fractions at the Surface of the PS/PMMA Blends Determined by XPS

	f_{MMA}			
takeoff angle (deg)	0.03	0.06	0.09	0.11
90	0.011	0.030	0.041	0.045
10	–	0.016	0.025	0.023

as the f_{MMA} increased to larger than 0.2, the annealed blends became hazy and no SF signal could be detected. The loss SF signal may be a result of scattering of light by the domains formed as a result of segregation of the immiscible PS and PMMA components.

The effect of annealing on the surface composition of the PS/PMMA blends was also examined by contact-angle and XPS measurements. The values of the water contact angle on annealed samples were nearly independent of f_{MMA} (solid circles in Figure 6) and close to that on the pure PS surfaces when f_{MMA} is smaller than 0.11. The increase of contact angles on these annealed samples indicates the surface of the blends was enriched with PS molecules. When f_{MMA} is higher than 0.13, the water contact angle values for the annealed sample decrease, indicating that the annealing time may be too short and the segregation process is not complete. More evidence of the PS surface segregation was also obtained from XPS results at both 90° and 10° takeoff angles. The PMMA surface concentrations in the annealed samples are calculated from eq 1, and the results are listed in Table 2. At a 90° takeoff angle, the ester carbonyl C 1s peak (289.0 eV) from PMMA is present for all the four samples, with generally a slight increase in PMMA content as the bulk PMMA mole ratio increased. At a 10° takeoff angle, under which the probe depth is ~4 nm, the PMMA concentration is smaller than the corresponding 90° measurements, indicating there are fewer PMMA molecules at the topmost layer. The XPS results confirm the migration of PMMA molecules from top layers of the RT-dried blends into the bulk of the blend after annealing at high temperature, whereas PS molecules preferentially segregate to the film surface. These results are consistent with those obtained by Ton-That et al.[5] They showed that >14 h annealing of a 50 wt % PS/PMMA blend resulted in a continuous PS-rich single phase on the blend surface. By comparing the experimental results of SF spectroscopy, contact-angle measurements and XPS, one may notice that although the contact angles and XPS results confirm that PS molecules predominate on the surfaces of the annealed blends, the SF peak in the PMMA region is still significant (Figure 7), suggesting that the ester methyl groups inside the blend are still SF active. It is also interesting to note from the SF spectra of the annealed PS/PMMA blends that the peak in the PMMA region occurs at ~2952 cm^{-1}, 8 cm^{-1} lower than that of the pure PMMA surfaces. The 2952 cm^{-1} peak has the same width as the 2960 cm^{-1} peak and corresponds to the shoulder seen in RT-dried samples (B in Figure 4). It is likely that this shift is a result of the environmental changes of the PMMA molecules experienced in the PS matrix because PS provides a more polar environment than air. The red shift of the ester methyl peak was also observed on a PS-on-PMMA bilayer constructed by sequentially spin-coating PMMA in $CHCl_3$ and PS in cyclohexane onto the substrate.[29] That experiment also confirms that the observed 2952 cm^{-1} peak of the annealed PS/PMMA blends originates from the ester methyl groups under the PS rather than the free surface of the polymer blends.[29] Because ultrathin polymer films are used in this study, all three interfaces (polymer−air, polymer−polymer, and polymer−substrate) are being probed simultaneously by SFG. Apparently, the SF spectrum depicted in Figure 5A,B contain SF features from both polymer−air and polymer−polymer interfaces. The broad feature in the PMMA region in Figure 5A is a result of unresolved 2952 and 2960 cm^{-1} resonances, and the 2952 cm^{-1} shoulder in Figure 5B originates from PMMA−PS interface. A schematic representation of a RT-dried PS/PMMA blend structure ($f_{MMA} < 0.06$) is shown in Figure 8. It should be noted that an internal PS−PMMA interface also exists in the RT-dried blends, whose structure can be qualitatively described as a bilayer.[5] If the ester methyl groups orient the same way as in the annealed blends, one would expect a polarization of opposite phase, which might result in a distortion of the 2960 cm^{-1} peak. However, no obvious asymmetry was observed from the SF spectra in Figure 5. Therefore, the lack of SF signals from the internal PS−PMMA interface suggests that it is more random than that in the annealed blends. One possible scenario is that the ester methyl groups bury themselves into the bulk PMMA phase within these RT-dried blends.

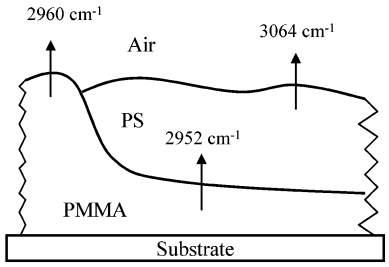

Figure 8. Schematic diagram of a cross-section along the surface normal of a RT-dried PS/PMMA blend.

Conclusions

Sum-frequency spectroscopy has been used to provide in-depth information about surface structures at both polymer−air and polymer−polymer interfaces of PS/PMMA blend films. SF results correlate well with those obtained by contact angle measurements and XPS. In addition, SF spectroscopy also revealed some unique information about the polymer thin layers. The PMMA phase dominates the blend surface after spin-coating from chloroform and vacuum-dried at RT. The PS molecules migrate to the surface upon annealing, whereas the ester methyl

groups of PMMA are found to retain their orientation within the annealed PS/PMMA blends.

Acknowledgment. This work was supported by the National Science Foundation (CHE-9875632). We thank Dr. A. C. Miller for the technical assistance with the XPS experiments. Y.L. acknowledges the Student Chemist Fellowship from Department of Chemistry, Lehigh University.

References and Notes

(1) *Polymer Surfaces and Interfaces III*; Richards, R. W., Peace, S. K., Eds.; John Wiley & Sons: Chichester, U.K., 1999.

(2) Garbassi, F., Morra, M., Occhiello, E., Eds.; *Polymer Surfaces: From Physics to Technology*, revised and updated ed.; John Wiley & Sons: Chichester, U.K., 1998.

(3) Andrade, J. D. *Polymer Surface Dynamics*; Plenum Press: New York, 1988.

(4) Ton-That, C.; Shard, A. G.; Teare, D. O. H.; Bradley, R. H. *Polymer* **2001**, *42*, 1121−1129.

(5) Ton-That, C.; Shard, A. G.; Daley, R.; Bradley, R. H. *Macromolecules* **2000**, *33*, 8453−8459.

(6) Tanaka, K.; Takahara, A.; Kajiyama, T. *Macromolecules* **1996**, *29*, 3232−3239.

(7) Tanaka, K.; Takahara, A.; Kajiyama, T. *Macromolecules* **1998**, *31*, 863−869.

(8) Wang, C.; Krausch, G.; Geoghegan, M. *Langmuir* **2001**, *17*, 6269−6274.

(9) Takahara, A.; Nakamura, K.; Tanaka, K.; Kajiyama, T. *Macromol. Symp.* **2000**, *159*, 89−96.

(10) Walheim, S.; Boltau, M.; Mlynek, J.; Krausch, G.; Steiner, U. *Macromolecules* **1997**, *30*, 4995−5003.

(11) Dutcher, J. R.; Wang, Z.; Neal, B. J.; Copeland, T.; Stevens, J. R. *Mater. Res. Soc. Symp. Proc. (Thin Films: Stresses and Mechanical Properties V)* **1995**, *356*, 535−540.

(12) Chen, Q.; Zhang, D.; Somorjai, G.; Bertozzi, C. R. *J. Am. Chem. Soc.* **1999**, *121*, 446−447.

(13) Chen, Z.; Gracias, D. H.; Somorjai, G. A. *Appl. Phys. B: Lasers Opt.* **1999**, *B68*, 549−557.

(14) Wang, J.; Chen, C.; Buck, S. M.; Chen, Z. *J. Phys. Chem. B* **2001**, *105*, 12118−12125.

(15) Wei, X.; Hong, S. C.; Lvovsky, A. I.; Held, H.; Shen, Y. R. *J. Phys. Chem. B* **2000**, *104*, 3349−3354.

(16) Gautam, K. S.; Schwab, A. D.; Dhinojwala, A.; Zhang, D.; Dougal, S. M.; Yeganeh, M. S. *Phys. Rev. Lett.* **2000**, *85*, 3854−3857.

(17) Chen, C.; Wang, J.; Woodcock, S. E.; Chen, Z. *Langmuir* **2002**, *18*, 1302−1309.

(18) Briggman, K. A.; Stephenson, J. C.; Wallace, W. E.; Richter, L. J. *J. Phys. Chem. B* **2001**, *105*, 2785−2791.

(19) Zhang, D.; Dougal, S. M.; Yeganeh, M. S. *Langmuir* **2000**, *16*, 4528−4532.

(20) Wang, J.; Woodcock, S. E.; Buck, S. M.; Chen, C.; Chen, Z. *J. Am. Chem. Soc.* **2001**, *123*, 9470−9471.

(21) Oh-e, M.; Lvovsky, A. I.; Wei, X.; Shen, Y. R. *J. Chem. Phys.* **2000**, *113*, 8827−8832.

(22) Miyamae, K.; Tsukagoshi, K.; Matsuoka, O.; Yamamoto, S.; Nozoye, H. *Langmuir* **2001**, *17*, 8125−8130.

(23) Miyamae, T.; Yamada, Y.; Uyama, H.; Nozoye, H. *Surf. Sci.* **2001**, *493*, 314−318.

(24) Wei, X.; Zhuang, X.; Hong, S.-C.; Goto, T.; Shen, Y. R. *Phys. Rev. Lett.* **1999**, *82*, 4256−4259.

(25) Gracias, D. H.; Chen, Z.; Shen, Y. R.; Somorjai, G. A. *Acc. Chem. Res.* **1999**, *32*, 930−940.

(26) Chen, Z.; Ward, R.; Tian, Y.; Eppler, A. S.; Shen, Y. R.; Somorjai, G. A. *J. Phys. Chem. B* **1999**, *103*, 2935−2942.

(27) Opdahl, A.; Phillips, R. A.; Somorjai, G. A. *J. Phys. Chem. B* **2002**, *106*, 5212−5220.

(28) Opdahl, A.; Phillips, R. A.; Somorjai, G. A. *Macromolecules* **2002**, *35*, 4387−4396.

(29) Liu, Y.; Messmer, M. C. *J. Am. Chem. Soc.* **2002**, *124*, 9714−9715.

(30) Harp, G. P.; Gautam, K. S.; Dhinojwala, A. *J. Am. Chem. Soc.* **2002**, *124*, 7908−7909.

(31) Chen, C.; Wang, J.; Even, M. A.; Chen, C. *Macromolecules* **2002**, *35*, 8093−8097.

(32) Huang, J. Y.; Shen, Y. R. In *Laser Spectroscopy and Photochemistry on Metal Surfaces*; Ho, W., Ed.; World Scientific: Singapore, 1995; pp 5−53.

(33) Bain, C. D. *J. Chem. Soc., Faraday Trans.* **1995**, *91*, 1281−1296.

(34) Eisenthal, K. B. *Chem. Rev.* **1996**, *96*, 1343−1360.

(35) Buck, M.; Himmelhaus, M. *J. Vac. Sci. Technol. A* **2001**, *19*, 2717−2736.

(36) Zhuang, X.; Miranda, P. B.; Kim, D.; Shen, Y. R. *Phys. Rev. B* **1999**, *59*, 12632−12640.

(37) Hirose, C.; Yamamoto, H.; Akamatsu, N.; Domen, K. *J. Phys. Chem.* **1993**, *97*, 10064−10069.

(38) Guyot-Sionnest, P.; Hunt, J. H.; Shen, Y. R. *Phys. Rev. Lett.* **1987**, *59*, 1597−1600.

(39) Chen, Z.; Ward, R.; Tian, Y.; Baldelli, S.; Opdahl, A.; Shen, Y.-R.; Somorjai, G. A. *J. Am. Chem. Soc.* **2000**, *122*, 10615−10620.

(40) Yang, Y. J.; Pizzolatto, R. L.; Messmer, M. C. *J. Opt. Soc. Am. B* **2001**, *17*, 638−645.

(41) Conboy, J. C.; Messmer, M. C.; Richmond, G. L. *J. Phys. Chem.* **1996**, *100*, 7617−7622.

(42) Liu, Y.; Wolf, L. K.; Messmer, M. C. *Langmuir* **2001**, *17*, 4329−4335.

(43) Löbau, J.; Wolfrum, K. *J. Opt. Soc. Am. B* **1997**, *14*, 2505−2512.

(44) Beamson, G.; Briggs, D. *High-Resolution XPS of Organic Polymers: The Scienta ESCA300 Database*; John Wiley & Sons: Chichester, U.K., 1992.

(45) Hofmann, S. In *Practical Surface Analysis*; Seah, M. P., Ed.; Wiley: Chichester, U.K., 1996.

(46) Clancy, T. C.; Jan, J. H.; Dhinojwala, A.; Mattice, W. L. *J. Phys. Chem. B* **2001**, *105*, 11493−11497.

(47) Lipschitz, I. *Polym.-Plast. Technol. Eng.* **1982**, *19*, 53−106.

(48) Dybal, J.; Krimm, S. *Macromolecules* **1990**, *23*, 1301−1308.

(49) Brinkhuis, R. H. G.; Schouten, A. J. *Macromolecules* **1991**, *24*, 1496−1504.

(50) Sutandar, P.; Ahn, D. J.; Franses, E. I. *Macromolecules* **1994**, *27*, 7316−7328.

(51) Willis, H. A.; Zichy, M. V. J. I.; Hendra, P. J. *Polymer* **1969**, *10*, 737−746.

(52) Nagai, H. *J. Appl. Polym. Sci.* **1963**, *7*, 1697−1714.

(53) Douglas, J. F.; Schneider, H. M.; Frantz, P.; Lipman, R.; Granick, S. *J. Phys. Condens. Matter* **1997**, *9*, 7699−7718.

(54) Mayes, A. M.; Russell, T. P.; Bassereau, P.; Baker, S. M.; Smith, G. S. *Macromolecules* **1994**, *27*, 749−755.